Effect of Temperature on Carrying Capacity of Concrete Columns Confined with Multi-layers of CFRP

***Manar Takla*[1)] *and Ihssan Tarsha*[2)]**

[1)] PhD Student, Structural Engineering Department, Faculty of Civil Engineering, AL-Baath University, Syria. E-Mail: Manar.takla@wpu.edu.sy
[2)] Professor, Structural Engineering Department, Faculty of Civil Engineering, AL-Wataniya Private University, Syria. E-Mail: ehsan.altarsha@wpu.edu.sy

ABSTRACT

FRP-reinforced polymers are widely accepted for use in civil engineering applications to strengthen constructions and apply confinement on concrete columns, thereby increasing their ductility and increasing their carrying capacity, as these materials are characterized by high tensile strength, high strength-to-weight ratio and high corrosion resistance,… etc. In addition, the exposure of reinforced concrete structures to fire is one of the most dangerous challenges that lead to great destruction and structural failure in addition to loss of life. With the development of computer simulation theories to study the behavior of elements and structures under the influence of different loads (static, dynamic, thermal,… etc.), it is possible to study the behavior of concrete columns under the influence of axial vertical and non-axial structural loads and compare the results with those of previous research, thus saving time, effort and cost instead of laboratory testing. Strengthening concrete columns with fiber-reinforced polymers (FRPs) has been studied extensively, but the majority of published studies have focused on circular columns. Most concrete columns in the field have square or rectangular cross-sections and resist eccentric loading as well. The objective of this study is to investigate the performance of square reinforced concrete (RC) columns, wrapped with carbon FRP subjected to elevated temperature; so, in this paper, an analytical study was conducted using the ANSYS Workbench program, which follows the finite element method, to determine the effect of layer number of CFRP on carrying capacity of concrete columns and to study the effect of external standard fire on concrete columns confined with CFRP. The numerical results were compared with experimental results as far as possible. The study revealed the accuracy of analytical models when compared to experimental studies. The results have shown that with increasing the layer number of CFRP, the carrying capacity of concrete columns will increase, with no benefit of increasing the number of CFRP layers to be more than 4, where polymer materials are sensitive to fire so that they need insulation.

KEYWORDS: Confinement, CFRP, Concrete columns, External fire, Carrying capacity, ANSYS Workbench.

INTRODUCTION

Reinforced concrete is the most common material used in structural systems in the world. The behavior of these structures and their failure modes have been extensively studied. The use of fiber-reinforced polymer (FRP) composites that are externally applied for strengthening reinforced concrete structures, such as beams, slabs and columns, has been implemented experimentally by many researchers and has been

Received on 18/11/2019.
Accepted for Publication on 27/1/2020.

applied in construction. A column is one of the essential elements in civil engineering structures that transmits loads from the upper levels to the lower levels and then to the soil through the foundations. During their service life, columns confined by CFRP can undergo deterioration caused by overloading, environmental effects, as well as exposure to exterior deteriorating factors, like fire, among other factors. Therefore, failure of the column system in any structure for any reason could lead to catastrophic effects on the entire building. In addition, the degradation of concrete strength due to short-term exposure to elevated temperature (fire) has attracted the attention of researchers and practitioners in the last decades, where the behavior of concrete exposed to fire depends on its mix composition and is determined by complex interactions during the heating process. Modes of concrete failure under fire exposure vary according to the nature of fire, loading system and type of structure.

BACKGROUND

FRP systems were developed as alternatives to steel plate bonding. Bonding steel plates to the tension zones of concrete members with adhesive resins were shown to be viable techniques for increasing flexural strength. This technique has been used to strengthen many bridges and high-rise buildings around the world. Because steel plates can corrode, leading to deterioration of the bond between steel and concrete and because they are difficult to install, requiring the use of heavy equipment, researchers have looked to FRP materials as an alternative to steel. Experimental work using FRP materials for retrofitting concrete structures was reported as early as 1978 in Germany. Research in Switzerland led to the first applications of externally bonded FRP systems to reinforce concrete bridges for flexural strengthening. FRP systems were first applied to reinforced concrete columns for providing additional confinement in Japan in the 1980s. Previous research and field applications for FRP rehabilitation and strengthening are described in ACI 440.2R-17 (2017). In Europe, the International Federation for Structural Concrete (FIB, 2001) published a bulletin for design guidelines, entitled "externally bonded FRP reinforcement for reinforced concrete structures". In recent years, research into FRP materials as reinforcement for concrete has been steadily increasing and a number of research gap analyses have been reported which suggest that FRP behavior under fire is a critical research need that must be addressed before these materials will see widespread use in buildings. For example, Karbhari et al. (2003) presented a durability gap analysis for fiber-reinforced polymer composites in civil infrastructures based on a series of workshops conducted by the Civil Engineering Research Foundation (CERF) and the Market Development Alliance (MDA) in the United States. Gap analysis provides a very instructive overview of the various concerns associated with FRP under fire. Therefore, the study of structural elements confined by carbon fiber and exposed to fire is an important topic in the field of civil engineering.

Model Generation

The ultimate purpose of finite element analysis is to recreate numerically the behavior of an actual engineering system. In other words, the analysis must use an accurate numerical model of a physical prototype. In the broadest sense, this model consists of the nodes, elements, material properties, real constants, boundary conditions and other features that are used to represent the physical system.

Structural Elements (Tarsha and Takla, 2017; ANSYS, 2015; SAS ANSYS, 2008)

Solid65 Element Description

SOLID65 is used for the 3-D modeling of solids with or without reinforcing bars (rebar). The SOLID65 is capable of cracking in tension and crushing in compression. In concrete applications, for example, the SOLID65 capability of the element may be used to model the concrete, while the rebar capability is

available for modeling reinforcement behavior. The element is defined by eight nodes having three degrees of freedom at each node: translations in the nodal x, y and z directions. Up to three different rebar specifications may be defined. The concrete element is similar to a 3-D structural solid, but with the addition of special cracking and crushing capabilities. The most important aspect of this element is the treatment of nonlinear material properties. The concrete is capable of cracking (in three orthogonal directions), crushing, plastic deformation and creep. Rebars are capable of tension and compression, but not shear. They are also capable of plastic deformation and creep.

The geometry, node locations and the coordinate system for this element are shown in Figure 1.

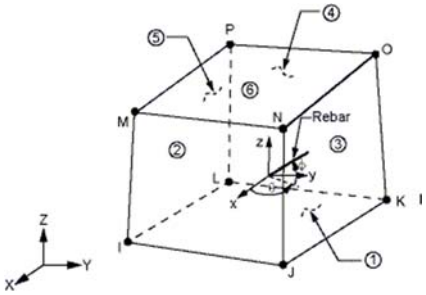

Figure (1): SOLID65 geometry

Link180 Element Description

ANSYS presents element LINK180 to accurately model reinforcing steel. LINK180 is a spar element that can be used in a variety of engineering applications. This element can be used to model trusses, sagging cables, links, springs, … etc. This 3-D spar element is a uniaxial tension-compression element with three degrees of freedom at each node: translations in the nodal x, y and z directions. As in a pin-jointed structure, no bending of the element is considered. Plasticity, creep, rotation, large deflection and large strain capabilities are included. The element is not capable of carrying bending loads. The stress is assumed to be uniform over the entire element. The geometry, node location and the coordinate system for this element are shown in Figure 2.

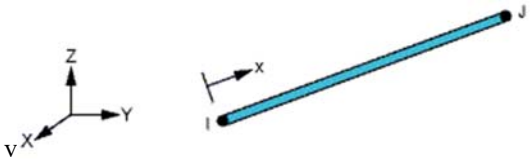

Figure (2): LINK180 geometry

Solid180 Element Description

This element could be used for 3-D modeling of solid structures. It is defined by eight nodes having three degrees of freedom at each node: translations in the nodal x, y and z directions. The geometry, node location and the coordinate system for this element are shown in Figure 3.

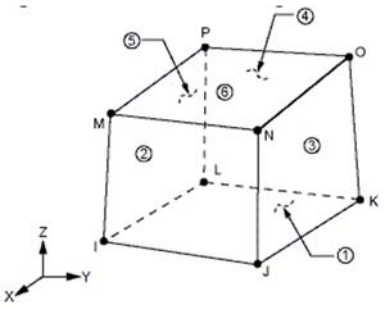

Figure (3): Solid180 geometry

Thermal Elements

Solid 70 Element Description

This element has a 3-D thermal conduction capability. The element has eight nodes with a single degree of freedom, temperature, at each node. The element is applicable to a 3-D, steady-state or transient thermal analysis. If the model containing the conducting solid element is also to be structurally analyzed, the element should be replaced by an equivalent structural element. This 8-node brick element is used, in this study, to simulate the behavior of concrete at thermal analysis. The geometry, node location and the coordinate system for this element are shown in Figure 4.

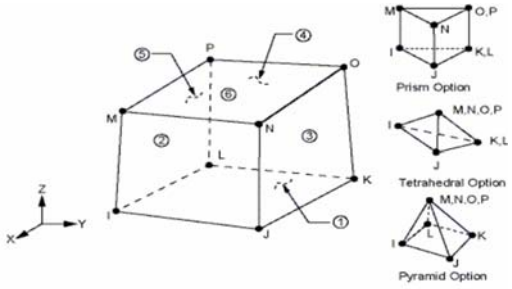

Figure (4): Solid70 geometry

Link 33 Element Description

This element is a uniaxial element with the ability to conduct heat between its nodes. The element has a single degree of freedom, temperature, at each node point. The conducting bar is applicable to a steady-state or transient thermal analysis. If the model containing the conducting bar element is also to be structurally analyzed, the bar element should be replaced by an equivalent structural element. This element is used, in this study, to simulate the behavior of steel reinforcement. The geometry, node location and the coordinate system for this element are shown in Figure 5.

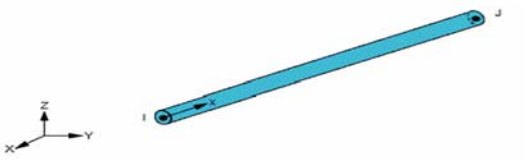

Figure (5): Link33 geometry

Structural and Thermal Analysis

The experimental model OCO (Hadi, 2012) was used to define the analysis parameters and compare experimental and analytical results. Material properties, model properties and thermal material properties are shown in Tables 1, 2 and 3, respectively.

Table 1. Material properties

Material Number	Element Type	Material Properties		
1	Solid65	**Linear Isotropic**		
		Young's modulus	47925 MPa	
		Poisson's ratio	0.2	
		Multilinear Isotropic		
			Strain	Stress (MPa)
		Point1	0.000497	23.50
		Point2	0.0009	37.28
		Point3	0.0014	52.93
		Point4	0.0017	60.59
		Point5	0.002	66.96
		Point6	0.0024	73.42
		Point7	0.0026	75.78
		Point8	0.0028	77.56
		Point9	0.003	78.77
		Point10	0.00332	79.5
		Concrete		
		Open shear transfer coef.		0.3
		Closed shear transfer coef.		0.8

		Uniaxial cracking stress	7.95
		Uniaxial crushing stress	-1
		Biaxial crushing stress	0
		Hydrostatic pressure	0
		Hydro biax crushing stress	0
		Hydro uniax crushing stress	0
		Tensile crack factor	0.6
2	**Link180**	**Linear Isotropic(S)**	
		Young's modulus	2.1e5 MPa
		Poisson's ratio	0.3
		Bilinear Isotropic(S)	
		Yield stress	516 MPa
		Tangent modulus	2100 MPa
		Linear Isotropic (L)	
		Young's modulus	2.1e5 MPa
		Poisson's ratio	0.3
		Bilinear Isotropic (L)	
		Yield stress	564 MPa
		Tangent modulus	2100 MPa
3	**Solid185**	**Linear Isotropic**	
		Young's modulus	2.1e5 MPa

Table2. Model properties

Model properties	
Cross-section (mm)	$(200 \times 200 \times 800)$
Compressive strength of concrete	79.5
Concrete cover (mm)	20
Yield strength of longitudinal steel reinforcement (MPa)	564
Yield strength of transverse steel reinforcement (MPa)	516
Diameter of longitudinal steel reinforcement (mm)	12
Diameter of transverse steel reinforcement (mm)	8

Table 3. Thermal material properties

Material properties for elements used in thermal analysis			
Number	**Element**	**Property**	**Value**
1	**Solid70**	Density [kg/m^3]	2300
		Specific heat [J]/ [kg].[K]	1100
		Conductivity [W]/[m].[K]	1.2
		Thermal expansion	1e-5
2	**Link33**	Density [kg/m^3]	7850
		Specific heat [J]/ [kg].[K]	700
		Conductivity [W]/[m].[K]	45
		Thermal expansion	1.3e-5

Results of Structural Analysis

The results of the analysis gave great accuracy after the completion of the numerical analysis of the reference model OCO (Hadi, 2012), where the ratio of the difference between failure loads determined analytically and experimentally was as follows:

- 0.9% for unconfined model.
- 0.73 % for columns with one layer of CFRP.
- 3.24 % for columns with three layers of CFRP.

Therefore, it can be considered that the analytical model agrees with the experimental model.

The results of structural analysis are included in Table 4 and Figures 6, 7, 8, 9, 10 and 11, respectively. Figure 12 shows the relationship between the number of carbon fiber layers and the carrying capacity of the columns. The compressive strength of the confined concrete results obtained from the analysis are shown in Table 5. As for Figure 13, it shows the relationship of the numbers of carbon fiber layers with the compressive strength of confined concrete (f_{CC}).

Table 4. Numerical results as obtained by ANSYS Workbench

Model	**Failure load (kN)**	
	Experimental (Hadi, 2012)	**Analytical**
C79.5-L12	-----	3160.7
C79.5-L12-S8	3248	3218.7
C79.5-L12-S8+1CFRP	3279	3255
C79.5-L12-S8+2CFRP	-----	3306.9
C79.5-L12-S8+3CFRP	3585	3468.7
C79.5-L12-S8+4CFRP	------	3479.7

C-concrete; L-longitudinal reinforcement; S-stirrups' reinforcement

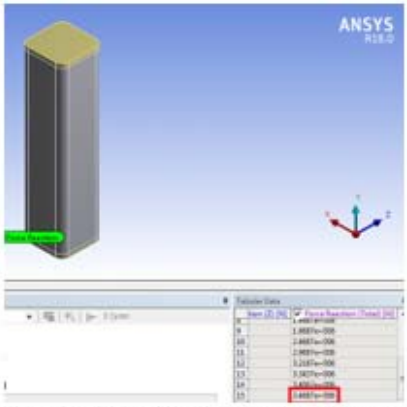

Figure (6): Failure load of model C79.5-L12

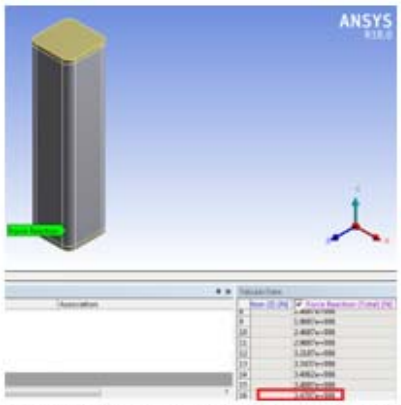

Figure (7): Failure load of model 79.5-L12-S8

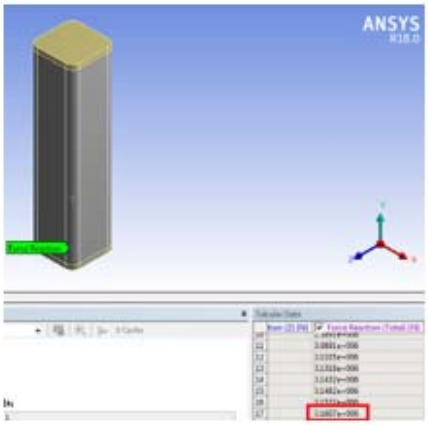

Figure (8): Failure load of model C79.5-L12-S8+1CFRP

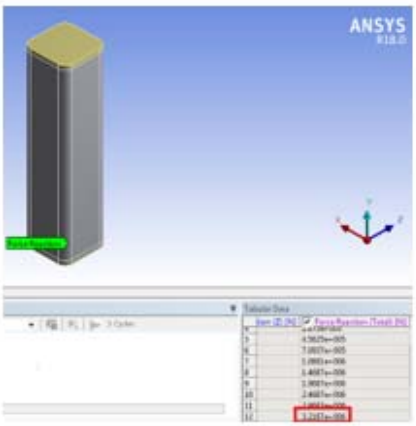

Figure (9): Failure load of model C79.5-L12-S8+2CFRP

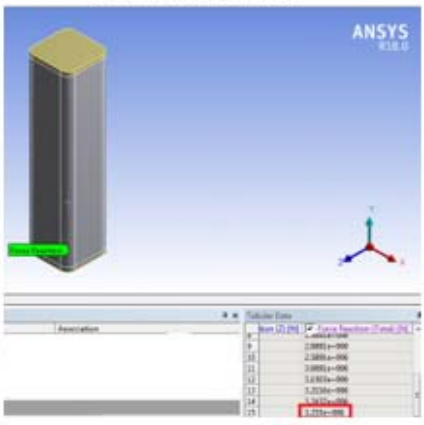

Figure (10): Failure load of model C79.5-L12-S8+3CFRP

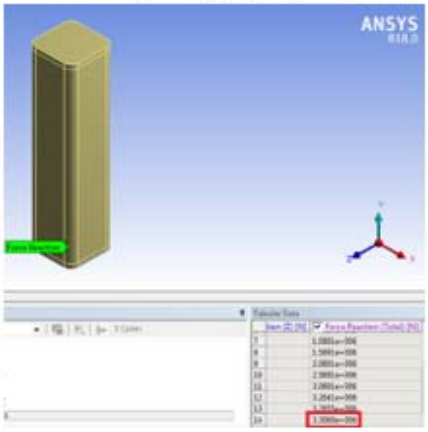

Figure (11): Failure load of model C79.5-L12-S8+4CFRP

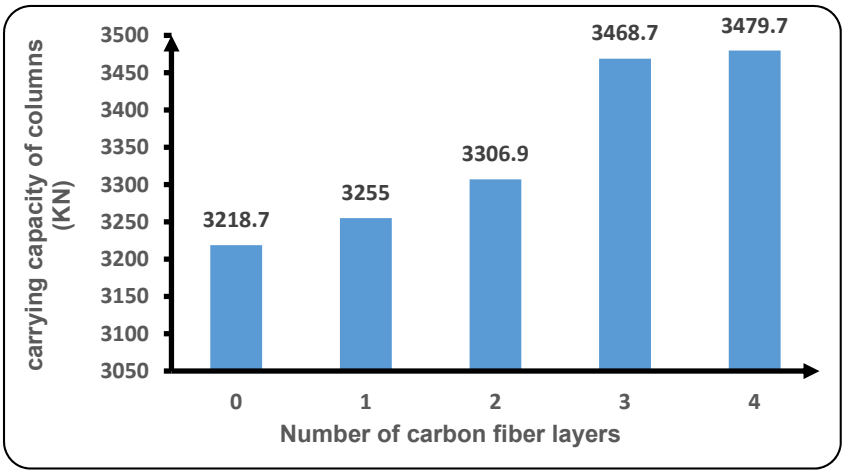

Figure (12): The relationship between the number of carbon fiber layers and the carrying capacity of columns

Table 5. Compressive strength of the confined concrete

The numerical results by ANSYS Workbench		
Model	**Failure load (kN)**	**Compressive strength of the confined concrete $f'_{cc}(MPa)$**
C79.5-L12	3160.7	82.06
C79.5-L12-S8	3218.7	
C79.5-L12-S8+1CFRP	3255	83.66
C79.5-L12-S8+2CFRP	3306.9	85.95
C79.5-L12-S8+3CFRP	3468.7	93.09
C79.5-L12-S8+4CFRP	3479.7	93.58

The compressive strength of the confined concrete was calculated as follows:

$$f'_{cc} = \frac{N_{cr}(C79.5 - L12 - S8) - N_{cr}(C79.5 - L12)}{A_{cc}} + f'_{c} \quad (1)$$

$$f'_{cc} = \frac{N_{cr}(C79.5 - L12 - S8 + n\ CFRP) - N_{cr}(C79.5 - L12)}{A_{cc}} + f'_{c} \quad (2)$$

where:

N_{cr}: Failure load (kN).

f'_{c} : Compressive strength of the concrete.

f'_{cc} : Compressive strength of the confined concrete.

A_{cc}: Area of the concrete within the center lines of the perimeter hoop.

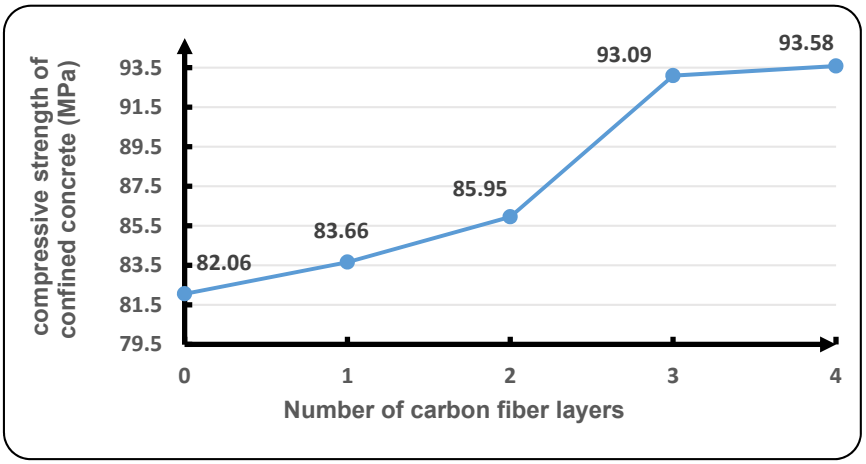

Figure (13): The relationship between the number of carbon fiber layers and compressive strength of confined concrete (f_{CC})

Thermal Structure Analysis (Tarsha and Takla, 2016; Tarsha and Takla, 2019; SAS ANSYS, 2008)

The analysis consists of two parts: thermal analysis to evaluate the fire temperature distribution inside the columns and structural analysis to evaluate its structural response, see Figure 14. The analysis was performed by using ANSYS Workbench computer program. The models were exposed to external fire from 4 sides. The equation of fire is given as:

$$T_g = 660 .(1 - 0.687 .e^{-0.32t} - 0.313 .e^{-3.8t}) + 20.$$

Thermal distribution at 60 minutes of model C79.5-L12-S8 is shown in Figure 15. As for Table 6 and Figure 16, they show the numerical results as obtained by ANSYS Workbench after thermal structure analysis.

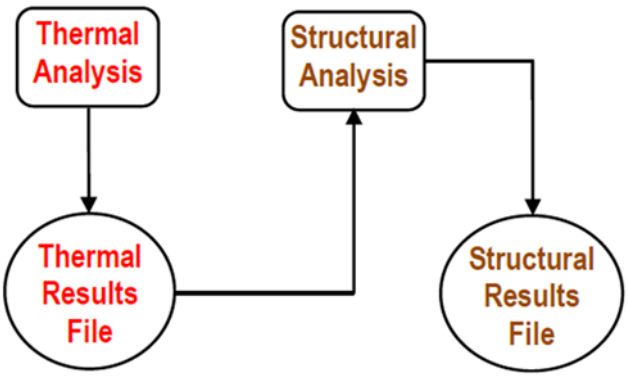

Figure (14): Analysis methodology

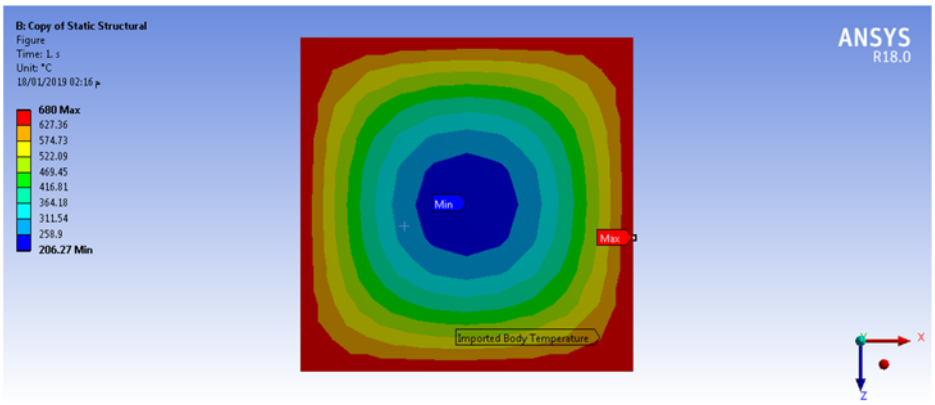

Figure (15): Thermal distribution at 60 minutes of model C79.5-L12-S8

Stress-Strain Curve for Concrete at Different Temperatures (Eurocode 4, 2005)

The stress-strain relationships given in Figure 16 are defined by two parameters:

- The compressive strength $f_{c,\theta}^{'}$;
- The strain $\varepsilon_{cu,\theta}$ corresponding to $f_{c,\theta}^{'}$.

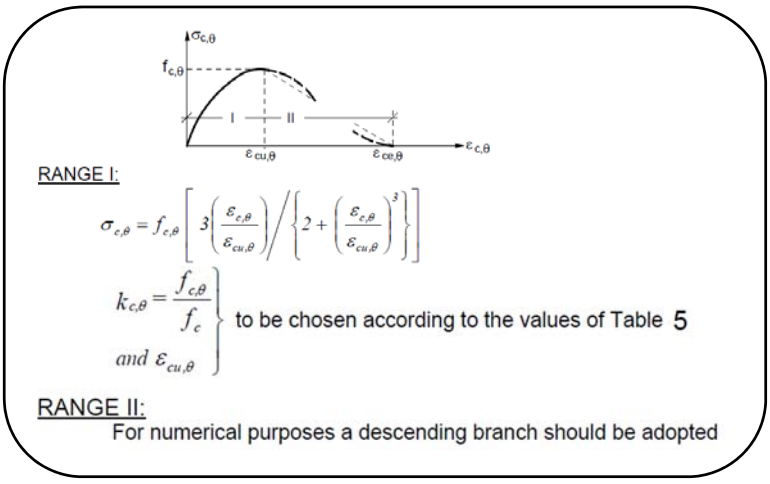

Figure (16): Mathematical model for stress-strain relationships of concrete under compression at elevated temperatures

Table 6. Values for the two main parameters of the stress-strain relationships of normal weight concrete (NC) and lightweight concrete (LC) at elevated temperatures

Concrete Temperature [ºC]θ_c	$K_{c,\theta} = f_{c,\theta}/f_c'$		$\varepsilon_{cu,\theta} \times 10^{-3}$ NC
	NC	LC	
20	1	1	2.5
100	1	1	4
200	0.95	1	5.5
300	0.85	1	7
400	0.75	0.88	10
500	0.6	0.76	15
600	0.45	0.64	25
700	0.3	0.52	25
800	0.15	0.4	25
900	0.08	0.28	25
1000	0.04	0.16	25
1100	0.01	0.04	25
1200	0	0	-

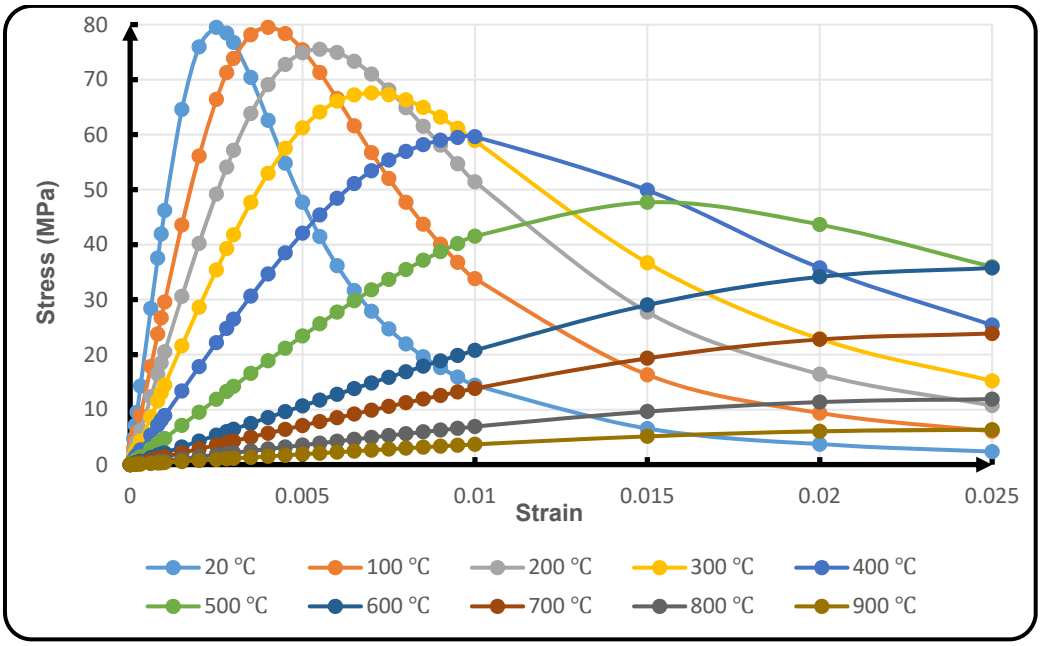

Figure (17): Stress-strain curves for concrete at different temperatures used in the program

Table 7. The numerical results as obtained by ANSYS Workbench after thermal structure analysis

Model	Analytical failure load after fire (kN)
C79.5-L12	2980.4
C79.5-L12-S8	2940.2
C79.5-L12-S8+1CFRP	2910.6
C79.5-L12-S8+2CFRP	2894.3
C79.5-L12-S8+3CFRP	2857.6
C79.5-L12-S8+4CFRP	2827.1

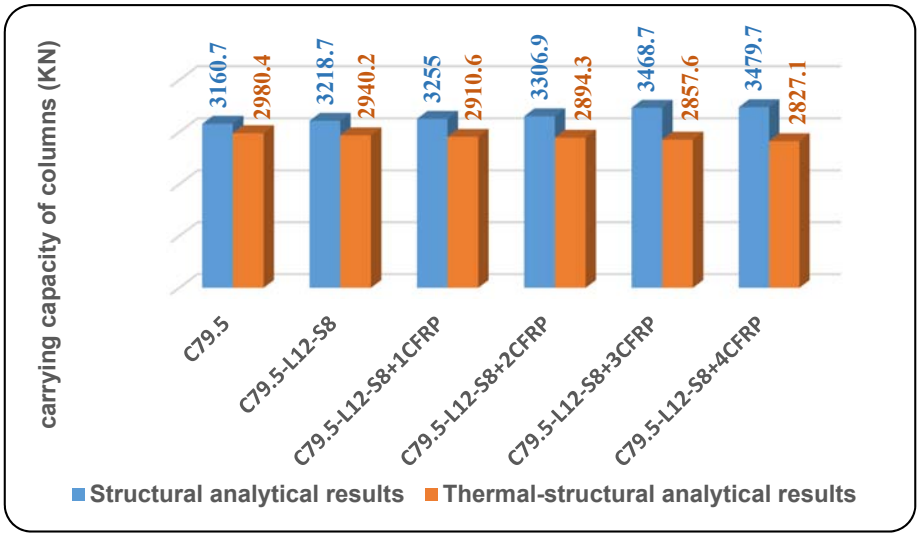

Figure (18): The numerical results as obtained by ANSYS Workbench

Discussion of Failure and Ultimate Carrying Load Capacity

- Carrying capacity of concrete columns decreased by about 9% after exposure to fire for 60 minutes.
- Carrying capacity of concrete columns confined with one layer of carbon fiber increased by 11% at the same time (t=60 minutes).
- Carrying capacity of concrete columns confined with two layers of carbon fiber increased by 12.5% at the same time (t=60 minutes).
- Carrying capacity of concrete columns confined with three layers of carbon fiber increased by 17.6% at the same time (t=60 minutes).
- Carrying capacity of concrete columns confined with four layers of carbon fiber increased by 19% at the same time (t=60 minutes).

CONCLUSIONS

1. By increasing the number of carbon fiber layers, concrete carrying capacity increases.
2. There is no great benefit in increasing the number of carbon fiber layers to be more than 3 layers.
3. Carbon fiber material is sensitive to heat and requires a heat insulating material.
4. Carbon fiber properties can be used to increase the

carrying capacity of concrete columns only if these fibers are protected from heat by insulating materials or by using thermal treatment fibers.

Recommendations

1. Conducting experimental studies and comparing the results of this research with the experimental results.
2. Using carbon fiber insulation materials when exposed to fire and investigating the effectiveness of these materials.

Acknowledgments

The authors would like to express their thanks and appreciation to Al Baath and Yarmouk Universities for supporting this research.

REFERENCES

ACI 318M-08. (2008). “Building code requirements for structural concrete and commentary”.

ACI 440. 2R-17. (2017). "Guide for the design and construction of externally bonded FRP systems for strengthening concrete structures”.

ACI Committee 440. (2008). “Guide for the design and construction of externally bonded FRP systems for strengthening concrete structures; ACI 440.2R-08”. American Concrete Institute: Farmington Hills, MI, USA.

ANSYS. (2015). “Manuals”.

Eurocode 4. (2005). “Design of composite steel and concrete structures, part 1-2: General rules-structural fire design.

FIB. (2001). “Externally bonded FRP reinforcement for RC structures”. FIB, Lausanne, 138.

Hadi, M.W. (2012). "Axial and flexural performance of square RC columns wrapped with CFRP under eccentric loading". Journal of Composites for Construction, 16 (6), 640-649.

Ihsan Tarsha, and Manar Takla. (2017). “Effect of fire on confined concrete columns under axial loading”. IISTE: International Knowledge Sharing Platform, 9 (9).

Ihssan Tarsha, and Manar Takla. (2016). “Ultimate load for composite column subjected to ISO 834 fire”. Journal of Al- Baath University, 38.

Ihssan Tarsha, and Manar Takla. (2019). Determination of failure load for structural elements exposed to fire and comparison to the design load according to Isotherm500 method”. Journal of Al Baath University, 41.

KarbharI, V.M., Chin, J.W., Hunston, D., Benmokrane, B., Juska, T., Morgan, R., Lesko, J.J., Sorathia, U., and Reynaud, D. (2003). “Durability gap analysis for fiber-reinforced composites in civil infrastructure”. Journal of Composites for Construction, 7 (3), 238-247.

SAS ANSYS 12. (2008). “Finite element analysis system". SAS IP, Inc, USA.